



UNIVERSITY OF LEEDS

This is a repository copy of *Rapid generation of reaction permeability in the roots of black smoker systems, Troodos ophiolite, Cyprus.*

White Rose Research Online URL for this paper:

<http://eprints.whiterose.ac.uk/84061/>

Version: Publishers draft (with formatting)

---

**Article:**

Cann, J, McCaig, AM and Yardley, BWD (2015) Rapid generation of reaction permeability in the roots of black smoker systems, Troodos ophiolite, Cyprus. *Geofluids*, 15 (1-2). 179 - 192. ISSN 1468-8115

<https://doi.org/10.1111/gfl.12117>

---

**Reuse**

Unless indicated otherwise, fulltext items are protected by copyright with all rights reserved. The copyright exception in section 29 of the Copyright, Designs and Patents Act 1988 allows the making of a single copy solely for the purpose of non-commercial research or private study within the limits of fair dealing. The publisher or other rights-holder may allow further reproduction and re-use of this version - refer to the White Rose Research Online record for this item. Where records identify the publisher as the copyright holder, users can verify any specific terms of use on the publisher's website.

**Takedown**

If you consider content in White Rose Research Online to be in breach of UK law, please notify us by emailing [eprints@whiterose.ac.uk](mailto:eprints@whiterose.ac.uk) including the URL of the record and the reason for the withdrawal request.

# Rapid generation of reaction permeability in the roots of black smoker systems, Troodos ophiolite, Cyprus

J. R. CANN, A. M. MCCAIG AND B. W. D. YARDLEY

SEE, University of Leeds, Leeds, UK

## ABSTRACT

The deep levels of former black smoker hydrothermal systems are widespread in the Troodos ophiolite in Cyprus. They are marked by zones of hydrothermal reaction in the sheeted dyke unit close to the underlying gabbros. These zones are characterized by the presence of epidote (epidote–quartz rock). In the reaction zones, the dykes are altered to a range of greenschist facies mineral assemblages, from a low degree of alteration with a five to seven phase metabasaltic assemblage to a high degree of alteration with a two to three phase epidote assemblage. Individual dykes may contain the full range, with the epidotes forming yellow–green stripes within a darker background, often extending for more than several metres, parallel to the dyke margins. Field relations show that the alteration took place on a dyke-by-dyke basis and was not a regional process. SEM petrography reveals that the epidotes contain millimetre scale pores. The minerals surrounding the pores show euhedral overgrowths into the free pore space, indicating a former transient porosity of up to 20%. We conclude that the epidotes formed by reaction between newly intruded basaltic dykes and actively circulating black smoker fluid leading to extensive dissolution of primary dyke minerals. This reaction generated the porosity in the stripes and transiently led to a much increased permeability, allowing the rapid penetration of the black smoker fluid into the dykes and flow along them in fingers. As the system evolved, the same flow regime allowed mineral precipitation and partial infilling of the porosity. This mechanism allows rapid recrystallization of the rock with release of metals and other components into the fluid. This explains the depletion of these components in epidotes and their enrichment in black smoker vent fluids and the relatively constant composition of vent fluids as fresh rock is continually mined.

Key words: epidote, hydrothermal, permeability, sheeted dikes, Troodos

Received 27 January 2014; accepted 22 September 2014

Corresponding author: Johnson R. Cann, SEE, University of Leeds, Leeds, LS2 9JT, UK.  
Email: j.cann@see.leeds.ac.uk. Tel: +44 1931 712429.

Geofluids (2014)

## INTRODUCTION

The transformation of cold sea water to hot black smoker fluid at oceanic spreading centres is one of the most dramatic of hydrological processes. A major black smoker vent field may emit 0.5–1 GW of thermal energy, corresponding to about 0.5–1 m<sup>3</sup> s<sup>-1</sup> of high-temperature fluid (Humphris & Cann 2000; Baker & German 2004; Di Iorio *et al.* 2012). Such flow may continue for long enough to generate major sulphide deposits containing up to several million tonnes of sulphides (Humphris & Cann 2000). Geophysical evidence from the East Pacific Rise and the Juan de Fuca Ridge is that the heat transfer to the circulating fluid takes place close to an underlying magma chamber at a depth of 1–2 km below the spreading axis (Detrick *et al.* 1987; Van Ark *et al.* 2007). Ocean drilling

and submersible observations (Francheteau *et al.* 1992) and the structure of ophiolites (Baragar *et al.* 1990) shows that this region is composed of sheeted dykes formed by the repeated intrusion of dykes into one another as spreading takes place.

In the numerical modelling of black smoker systems, one critical problem has been the nature of a permeability structure of the crust that must consistently allow a high-heat output at a high temperature (Lowell & Germanovich 2004; Driesner 2010; Ingebritsen *et al.* 2010). Although modellers have used many approaches, developing over time, all models require a crustal permeability structure within the regions of hydrothermal circulation that is very closely defined. Their permeability estimates are significantly higher than the limited data set of *in situ* measurements in sheeted dykes from ODP Hole 504b (Becker &

Davis 2004), suggesting that ridge crest permeability is transient. What processes control the permeability structure and its evolution so closely?

Almost all authors assume that permeability in the ocean crust is largely controlled by fracturing, either as a result of cooling and thermal contraction (Lister 1974), or tectonic faulting and fracturing (Scott *et al.* 1974; German & Lin 2004). In this study, we document an additional mechanism, the creation of connected porosity by mineral dissolution in hydrothermal fluid. This mechanism for generating permeability is well known in karst and other diagenetic systems and has been suggested for skarns and marbles (Yardley & Lloyd 1989; Yardley *et al.* 1991; Balashov & Yardley 1998), but textural evidence has not previously been documented in black smoker systems.

The key lies in the direct investigation of the regions within which the hot, metal-bearing hydrothermal fluid circulates through the crust and rises to the ocean floor. Active regions of this kind are not accessible to direct investigation in the oceans by drilling, and fossil regions have been elusive in drill holes that have penetrated deep into older ocean crust, but they are exposed in ophiolites such as the Troodos ophiolite in Cyprus and the Semail ophiolite in Oman. In this study, we re-examine the processes that shape the zones of high-temperature hydrothermal alteration in the Troodos ophiolite through a combination of field evidence, petrography and chemistry, with the aim of understanding the links between alteration and fluid flow. In particular, we investigate the permeability structure that allowed the flow of fluid to take place through the reaction zone and its origin in the metasomatic reactions that conditioned the chemistry of the fluid. We show that mineral dissolution and creation of new porosity occurred during these metasomatic reactions, and occurred rapidly, between intrusion of one dyke and the next.

## THE TROODOS OPHIOLITE: GEOLOGICAL SETTING

A general introduction to the hydrothermal systems of the Troodos ophiolite of Cyprus can be found in Cann & Gillis (2004). Zones of high-temperature hydrothermal alteration are especially well exposed in the ophiolite, formed at a Cretaceous spreading centre above a subduction zone in a back arc environment (Pearce *et al.* 1984). This ophiolite extends for more than 100 km across the strike of the ancient spreading centre and contains remarkably complete units of the upper crust that have been affected only by low-temperature alteration since they formed (Staudigel *et al.* 1986; Gallahan & Duncan 1994). The ophiolite is capped by a unit of submarine lavas containing more than 30 sulphide deposits (Bear 1963; Adamides 1990) similar to those found associated with oceanic black smoker

systems (Humphris & Cann 2000) and containing fossilized vent organisms (Little *et al.* 1999). Beneath the lavas is a unit of sheeted dykes that overlies a unit of gabbro formed by crystallization of the axial magma chamber (Fig. 1).

Most of the thickness of the sheeted dyke unit in the ophiolite is made up entirely of dykes intruded at the ancient spreading centre. The dykes intrude one another and are marked by well-defined chilled margins. They range in thickness from a few tens of centimetres up to a few metres. In every outcrop, there are some late dykes that are preserved complete with two chilled margins, but most of the outcrop is of dykes that have been intruded by other dykes, often in several stages. These earlier dykes are present as elongate lenses, sometimes with one chilled margin, at other times without a chilled margin visible. Careful field observations show that most lenses without chilled margins have a chilled margin on a segment of the dyke

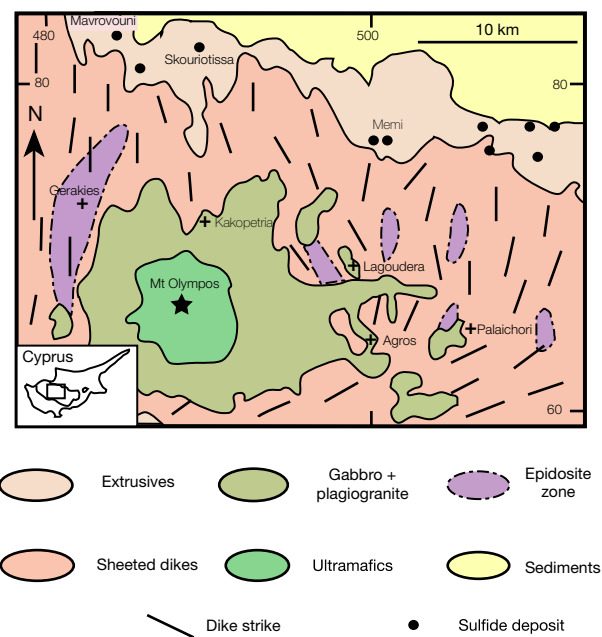


**Fig. 1.** Outline geological map of the central part of the Troodos ophiolite. The ophiolite is in the form of a dome. The deepest parts of the section are the ultramafics, gabbros and plagiogranites, which are overlain by sheeted dykes, and in turn by volcanics. The overlying sediments include deep ocean chalcs and more recent deposits. The epidote zones lie close to the base of the sheeted dyke unit, except for the northern end of the big western zone, including the Gerakies localities, which reaches close to the volcanic unit, though there accompanied by outcrops of gabbro (Bettison-Varga *et al.* 1995). The variable dike strike reflects the complex processes of crustal generation at the ancient spreading centre. For a general introduction to the ophiolite, explaining this and other features, see Edwards *et al.* (2010). The grid numbers are UTM coordinates using the WGS84 grid, truncated by removing the first two digits and the last three digits of both eastings and northings. Place names are selected villages as well as the highest point, Mount Olympos. The sulphide deposits are all within the volcanic sequence. Three of them are named.

on the other side of one of the intruding dykes (Kidd & Cann 1974); see Fig. 2. Although dykes are generally nearly parallel to one another, in most outcrops, there are some dykes that cut obliquely across others.

The dykes were intruded in a narrow zone at the ancient spreading centre. Modelling based on detailed field observations in Troodos (Kidd 1977) indicated that this zone might be as narrow as a few tens of metres. In the oceans, the zone of intrusion is marked by a chain of fissuring along the spreading axis that is about 200 m wide (Crane 1987). From this intrusion zone, the completed sheeted dyke complex was rafted off laterally by spreading.

Throughout most of the thickness of the sheeted dyke unit, the dykes have been metamorphosed to a typical greenschist facies assemblage: albite, actinolite, chlorite, quartz, epidote and titanite. This assemblage is referred to as the background alteration in what follows. Some parts of the sheeted dyke unit have been rotated by up to tens of degrees. This rotation occurred after the metamorphism was complete (Varga *et al.* 1999).

## EPIDOSITE ZONES: PREVIOUS WORK

Towards the lower part of the sheeted dyke unit are complex zones marked by the presence of epidosite (epidote–quartz rock), formed by profound chemical and mineralogical transformation of the dykes, set within dykes showing less profound alteration.

These ‘epidosite zones’ are typically a few hundred metres wide perpendicular to the strike of the dykes and extend for a kilometre or more parallel to the dyke strike. They have formed by alteration of the sheeted dykes, as the chilled margins and the intrusive relations of the dykes are well-preserved in outcrop. The mineral assemblages within the epidosite zones are much more variable than in the background sheeted dykes. Some of the dykes show the five to seven phase greenschist facies metadiabase assemblage of the background, but many of the dykes contain fewer phases. At the most extreme degree of alteration, the assemblage is the classic epidosite assemblage of epidote, quartz and either titanite or Fe oxides. At a somewhat less extreme degree of alteration and more abundant than true epidosites are epidote, chlorite, quartz and titanite (CQE) rocks. The degree of alteration varies on a small scale within and between dykes, so that a single dyke 2 m wide may contain thin stripes of epidosite at least several metres long, spaced 10–20 cm apart, associated with stripes of CQE rock, and set in a variable matrix containing regions with a larger number of phases including CQE assemblages (Jowitt *et al.* 2012).

The epidosites in Troodos were first identified during the earliest detailed geological survey of the ophiolite (Wilson 1959). Later work showed that the sulphide deposits of the ophiolite had formed by exhalation of hydrothermal fluid at the ocean floor (Constantinou & Govett 1972, 1973) pre-dating the discovery of active black smokers in

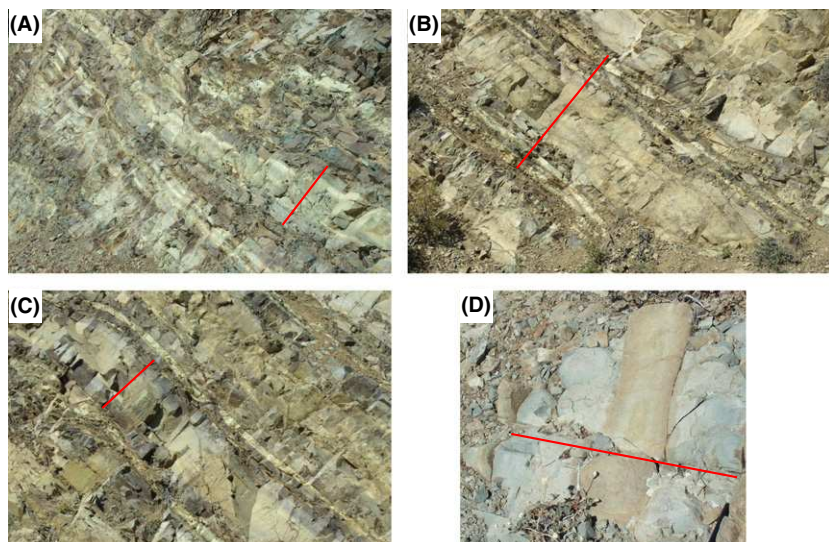


**Fig. 2.** Field photographs of epidosite zone exposures. Location references are UTM coordinates using the WGS84 grid, truncated by removing the first two digits of both eastings and northings. Red lines show the width of a prominent individual dike in each image. (A) Exposure of epidosite zone rocks showing the variety of colours in a single outcrop (exposure about 3 m high) (482160 68520). The paler lithologies are epidosites, and the darker colours are less altered dykes. (B) Striped dyke 1.5 m wide showing the symmetrical pattern of striping typical of wider dykes (481873 68871). (C) Dyke 0.7 m wide with a simpler alteration pattern. At the margins are narrow stripes of epidosite (481873 68871). The core of the dyke is more altered than the outer zones inside the epidosite stripes. (D) Incipient alteration shown by a pod, 0.2 m wide, of more highly altered rock inside a less altered dyke matrix (498774 67931).

1979. Detailed work began on the epidosites in the 1980s (Richardson *et al.* 1987; Schiffman *et al.* 1987).

It was recognized (Richardson *et al.* 1987) that the extreme phase reduction of the epidosites might be the product of intense metasomatic alteration of the dykes under open-system conditions as envisaged by Korzhinskii (1959, 1965). After their discovery in Troodos, epidosites were identified and described in several other ophiolites, the Josephine ophiolite in California/Oregon (Harper *et al.* 1988 and related papers), the Semail ophiolite in Oman (Nehlig & Juteau 1988; Nehlig *et al.* 1994) the Pindos ophiolite in Greece (Valsami & Cann 1992) and the Solund ophiolite in Norway (Fonneland-Jorgensen *et al.* 2005). Epidosites have only rarely been found in the modern oceans, but have been dredged from the fore arc of the Tonga Arc (Banerjee *et al.* 2000; Banerjee & Gillis 2001) and have been reported in rocks dredged from the Mid-Atlantic Ridge at 30°N (Shand 1949; Quon & Ehlers 1963).

Previous work on epidosites clarified a number of issues. The major element chemistry of rocks from epidosite zones shows the wide range in composition expected from the changing mineralogy (Richardson *et al.* 1987; Harper *et al.* 1988; Nehlig *et al.* 1994; Bettison-Varga *et al.* 1995). All of the rocks within epidosite zones, including the whole range from diabase to epidosite, are strongly depleted in Cu, Zn and Mn by between 50% and 90%, with Cu the most depleted and Mn the least (Richardson *et al.* 1987; Harper *et al.* 1988; Nehlig *et al.* 1994; Bettison-Varga *et al.* 1995). Jowitt *et al.* (2012) demonstrate both the spatial scale of mineral assemblages and the extent of metal depletion, including Ni as well as Cu, Zn and Mn. In contrast, Sr is enriched in the epidosites and  $^{87}\text{Sr}/^{86}\text{Sr}$  ratios are strongly altered both in epidosites, and surrounding dykes showing more typical greenschist facies assemblages, with values of ~0.705, intermediate between fresh basalt and Cretaceous sea water (Bickle & Teagle 1992; Bickle *et al.* 1998). Recent alteration of diabase in ODP Hole 504B is much less intense than that seen in Troodos (Teagle *et al.* 1998). Fluid inclusions within the epidosite zones, including all rock types, show homogenization temperatures broadly within the range 250–400°C, and salinities typically ranging from sea water to twice sea water concentrations (Richardson *et al.* 1987; Nehlig *et al.* 1994; Bettison-Varga *et al.* 1995; Juteau *et al.* 2000). Oxygen isotopes give evidence of extensive water–rock reaction at similar temperatures (Harper *et al.* 1988; Schiffman & Smith 1988; Nehlig *et al.* 1994; Fonneland-Jorgensen *et al.* 2005). All previous studies conclude from this evidence that epidosite zones have been the sites of intense hydrothermal interaction between black smoker fluids and dyke rock, with the true epidosites within them representing the places where fluid–rock interaction has been most intense.

There have been two end-member models of the generation of the high permeability in the rocks that allowed the intense fluid flow to take place. One is that permeability has been related to generation of fractures in the rocks by tectonic processes at the spreading centre (Bettison-Varga *et al.* 1992; Nehlig *et al.* 1994). The other is that the replacement of lower density silicates by dense epidote has generated porosity within the rocks and hence higher permeability. This concept has been referred to in passing by a number of authors (Harper *et al.* 1988; Nehlig & Juteau 1988; Bettison-Varga *et al.* 1992; Bickle *et al.* 1998), but only Bettison-Varga *et al.* (1995) have developed the model. No previous authors have given textural evidence for reaction porosity generation in epidosites.

This study extends the previous work in Troodos and other ophiolites in two directions. First, we report a detailed study of field relationships in the epidosite zones of Troodos. Second, we discuss new petrographic studies of Troodos epidosites, using scanning electron microscopy and cathodoluminescence.

## RESULTS

### Field relationships of epidosites

The progressive alteration of the mineral assemblages in the sheeted dykes, from background metabasaltic greenschist assemblages to epidosites, can be seen in excellent roadside exposures through the varying colour of the altered dykes (Fig. 2A). Precise field localities for examining epidosites may be found in Edwards *et al.* (2010) and localities are also given in the figure captions in this study. Epidosite, representing the highest degree of alteration, is a very pale greenish yellow, while rocks at a lower degree of alteration, with a greater content of chlorite and/or actinolite, are darker coloured reaching a dark bluish green where the content of quartz and epidote is low. This contrast in colour allows the spatial variation in mineral assemblage to be recorded in field photographs. The mineral assemblages vary from dyke to dyke and on a smaller scale within dykes. Individual dykes can be recognized by their chilled margins and the cross-cutting jointing typical of dykes in general, and these are preserved to the highest degrees of alteration.

Within individual dykes at higher degrees of alteration, the alteration is frequently striped parallel to the dyke margins, with stripes at a higher degree of alteration alternating with stripes of a lower degree. The edges of the stripes are often sharp, within a few millimetres. The pattern of striping is commonly symmetrical about the centre of the dyke, varying with the width of the dyke (Fig. 2B). Narrow dykes, up to a metre wide, commonly have a broad higher degree stripe down the centre and may have a narrow stripe of higher alteration close to the margin

(Fig. 2C). Wider dykes commonly contain several stripes of higher alteration close to the margin, separated by darker, wider stripes of lower alteration. The centres of dykes are commonly more altered than the regions close to the margins. Dykes at a lower degree of alteration may contain pods of a higher alteration elongate parallel to the dyke margins. These are inferred to have finger-like geometries in three dimensions (Fig. 2D).

The joints cutting dykes within epidote zones are only rarely filled with epidote and quartz. Most joints are empty of hydrothermal minerals. Epidote–quartz veins are commoner along dyke margins but are still not abundant. The rarity of alteration associated with the cross-cutting joints indicates that most of the alteration predates the jointing.

Cross-cutting dykes show three important features (Fig. 3). (i) Where one striped dyke crosses another, the margin of the younger dyke cuts across the stripes in the older dyke. These terminate at the margin of the younger dyke and reappear on the other side of it. The stripes in the younger dyke follow the bends in the dyke margin and remain parallel to each other. (ii) The degree of alteration of the older dyke does not change as it approaches the margin of the younger dyke. (iii) Dykes that are more altered frequently cut dykes that are less altered, which would not be expected if progressive alteration affected the whole dyke injection zone. All of these features indicate that the alteration occurred in one dyke at a time, while the physical nature of each dyke was distinct.

At a larger scale, epidote zones can be distinguished from background sheeted dykes by the presence of striped dykes in outcrops. Individual epidote zones are typically a few hundred metres wide and separated from each other by a few kilometres. They are best developed in the lower parts of the sheeted dyke unit, but in the area west of the Solea Graben reach higher structural levels close to the major sulphide deposits at Mavrovouni and Skouriotissa (Fig. 1) although there they are associated with outcrops of gabbro (Bettison-Varga *et al.* 1995).

### Petrography and mineral chemistry of epidotes

Samples from an epidote zone can be put in a broad series of decreasing number of mineral phases, although this does not necessarily imply a sequence of development. The background dykes from outside the epidote zones and many of the dykes within an epidote zone show a typical metabasalt greenschist facies assemblage of albite (with some relict calcic plagioclase), actinolite (with some relict clinopyroxene), chlorite, quartz, epidote, iron oxides and titanite. Their texture is a typical ophitic to subophitic igneous texture dominated by albite laths. As the degree of alteration increases and the number of mineral phases decreases, minerals drop out regularly. Typically albite disappears first, followed by actinolite. Chlorite is the next to go, although it survives to a high degree of alteration, and may reappear as a late phase at high degrees of alteration. At the highest degree of alteration, in the epidotes, the

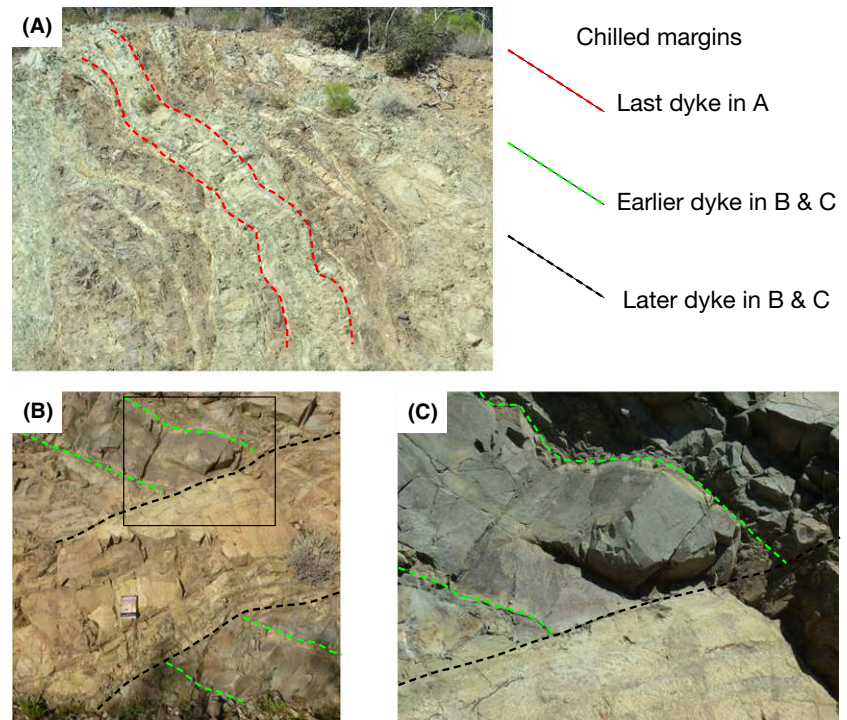


**Fig. 3.** Field photographs showing the relationships between dykes in an epidote zone. (A) A single highly altered dyke 1 m wide cutting through a complex of earlier dykes altered to different degrees. (B) A striped epidote dyke 1.5 m wide at a high degree of alteration, cutting a narrow 0.7-m-wide dyke at a lower degree of alteration and displacing its outcrop. (C) Enlarged view of the area outlined in B. Note the abrupt truncation of the earlier dyke and its marginal and central stripes by the later dyke and the apparent lack of any further alteration of the earlier dyke by the higher degree of alteration of the later one.

assemblage is quartz, epidote and titanite or iron oxide, a true epidosite. At this stage, alteration is no longer pseudomorphic and no trace of igneous texture remains.

The modal compositions of the true epidosites established by point counting are close to 30% quartz, 55% epidote and smaller amounts of titanite and voids. Less highly altered rocks with a significant amount of chlorite contain about 30% quartz, 35% epidote, 25% chlorite and small amounts of other phases such as actinolite, Fe oxides, titanite and void space.

The texture of the epidosites is pervasively granoblastic (Fig. 4). The grain size varies with the position in the dykes, and hence with the original igneous grain size, suggesting some memory of the original igneous texture. The proportions of epidote and quartz may vary over a single polished block from areas where quartz is more abundant than epidote to areas in which epidote is dominant. In many cases, the eventual grain size of the quartz is much greater than that of the epidote, with small subprismatic crystals of epidote included within larger quartz crystals (Fig. 5).

Most of the epidosites contain voids, some more or less equant, and in other cases, a network of cracks on a scale of a few millimetres, each crack around 0.1 mm wide. These void spaces are commonly fringed by euhedral terminations of the bordering crystals, indicating that adjacent

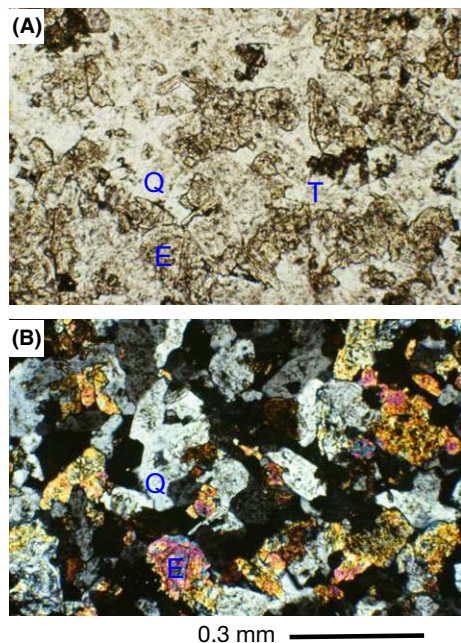


**Fig. 4.** Thin section photomicrograph of an epidosite in plane polarised light (A) and crossed polars (B), showing the absence of any relict igneous texture. The section shows epidote E, quartz Q and titanite T. The rock specimens in Figs 4–9 come from the road section west of Gerakies between (480830 73370) and 480940 73010).

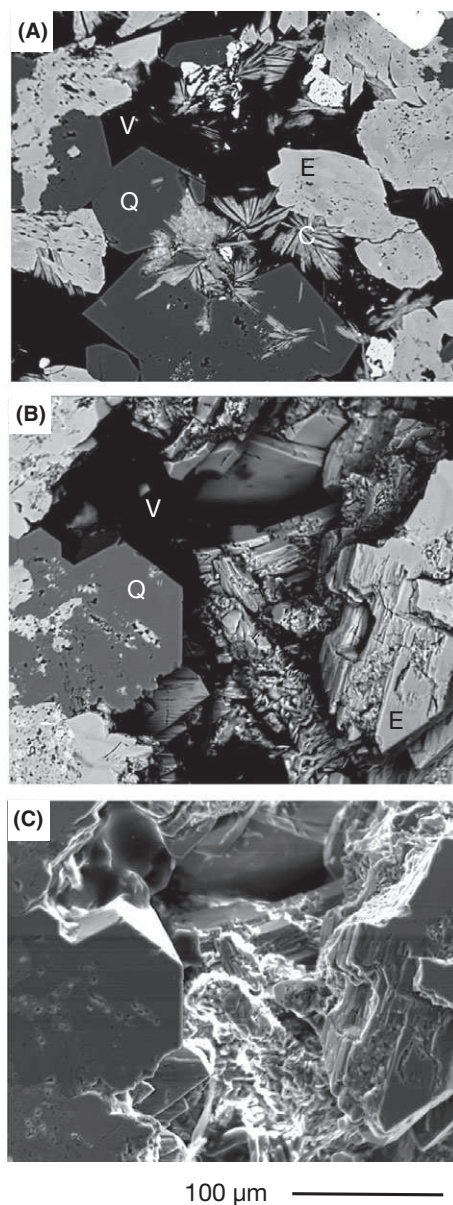


**Fig. 5.** Scanning electron microscope (SEM) images showing the relations between epidote (E), quartz (Q), chlorite (C) and the void spaces (V). (A) (58503) back-scattered electron (BSE) image. (B) (58519) back-scattered electron image. (C) Secondary electron image of the same area as B, showing euhedral grain facets within the pore. Epidote, quartz and chlorite are all clearly growing at least in part into porosity. Five-digit numbers in Figs 5, 7, 8 and 9 are University of Leeds specimen numbers.

crystals were growing into open space until the filling of the voids was been interrupted (Fig. 6).

Typically there is a variation in the texture within the matrix. Some regions show traces of the original igneous texture, often seen best in the scattered presence of pseudomorphs in titanite or magnetite of original Fe-Ti oxides. In other regions, any sign of igneous texture is lacking, and instead, there are replacive or space-filling textures

shown by optical zoning or trains of inclusions. This variation is typically on a scale of a few millimetres.

Back-scattered electron (BSE) images of polished surfaces show voids and the euhedral terminations of epidote and quartz at the edges of the voids. They also show that the crystals forming the euhedral fringe to the voids are free of inclusions. Areas of similarly inclusion-free crystals within the samples are interpreted to indicate the former presence of voids, now filled (Fig. 7).

Cathodoluminescence (CL) images (Connell 2000) of coarse quartz close to voids shows a clear growth zoning in CL, with bright zones and dark zones alternating parallel to crystal terminations (Fig. 8). The pattern of zoning is similar in samples from the same dyke and often different between dykes close together in the same outcrop. Some patterns show a CL-bright zoned core to crystals, a dark rim to crystals and late dark veins that cut across bright areas (Fig. 8). Other patterns show a dark zoned

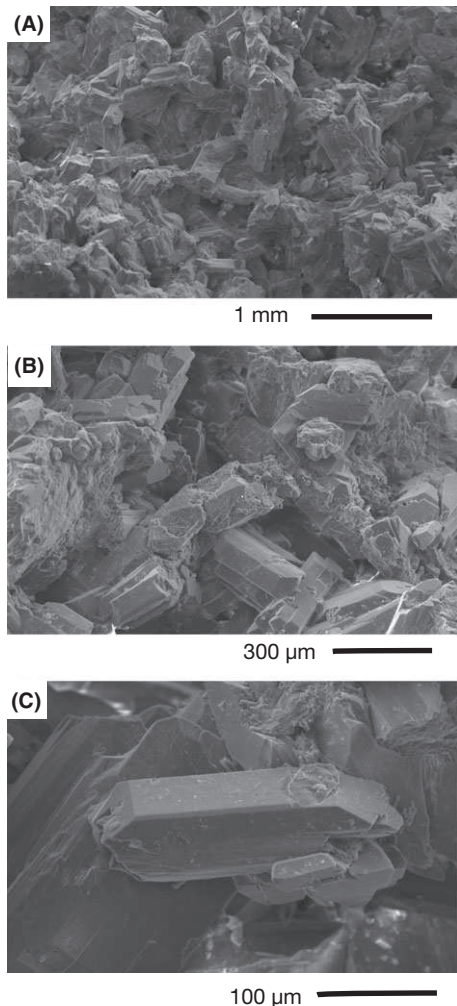


**Fig. 6.** SEM images of epidote surfaces broken in the laboratory, showing euhedral crystals of quartz and epidote fringing the void spaces.

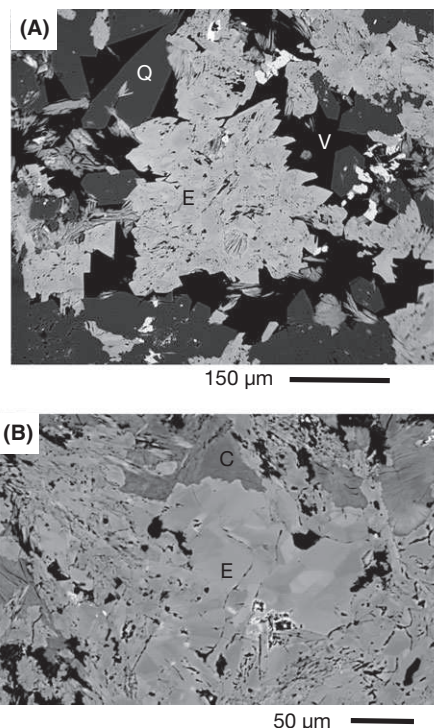


**Fig. 7.** SEM back-scattered electron images of polished specimens. (A) (58503) Cluster of epidote (E) and quartz (Q) crystals growing into void space (V). Note the euhedral terminations of the crystals towards the void. Note too the inclusion-free rims to the epidote crystals surrounding cores that are full of inclusions. Most of the inclusions are extremely small voids. (B) (58602) Coarse epidote crystals free of inclusions that have totally filled a void, growing from surrounding inclusion-rich crystals. The chlorite (C) appears to be late and to be corroding and replacing the epidote. The variation in brightness of the epidote crystals is the result of varying chemical composition ranging from  $\text{Al}/(\text{Al}+\text{Fe})$  0.85 to 0.80. Small euhedral cores can be seen within the inclusion-free epidote.

core, rimmed by a thin bright zone, rimmed again by a dark outer zone (Fig. 9). Electron probe traverses (Connell 2000) across zoned quartz shows that Al and Ti are enriched in the brighter zones (up to 1000 and 700 ppm, respectively) dropping to close to the detection limit in darker zones and late veins, while Fe is enriched from 1000 to 5000 ppm from the core to the margins of the crystals. Application of the Ti-in-quartz geothermometer (Wark & Watson 2006) gives meaningless temperatures which can exceed 1000°C, probably reflecting fast disequilibrium quartz precipitation (Huang & Audébat 2012). The associated epidote in areas close to voids is also zoned, as can be seen in the BSE images (Fig. 9). The epidote composition in such zoned crystals varies on a scale of a few tens of micrometres from  $\text{Al}/(\text{Al} + \text{Fe})$  0.7 to 0.85 (Connell 2000).

Samples taken from the epidote stripes are especially rich both in existing voids and in the evidence that these voids were once larger than now. There is a continuum

between clear evidence for void filling, and the more subtle textures suggesting that such void filling may have occurred in nearby coarser-grained areas. These include a common contrast between inclusion-rich cores to epidote-rich regions and wide inclusion-free rims adjacent to remaining voids. The voids would have been larger than any that now remain, perhaps reaching sizes of 5–10 mm and are inferred on the basis of the clear zones of epidote crystals and correlatable CL zones in quartz to have occupied volumes of up to 20% of the rock volume. Growth of euhedral crystal faces accompanied by fluctuations in mineral composition such as oscillatory zoning has been shown by Yardley *et al.* (1991) to be indicative of infiltration metasomatism.

## DISCUSSION

### Significance of epidote stripes

The association of the formation of epidosites with the circulation of black smoker fluid is inferred from a number of lines of evidence. The fluid inclusion data, the alteration mineral assemblages and the removal of Cu, Zn and Mn from the epidosite zones all coincide, as does the presence

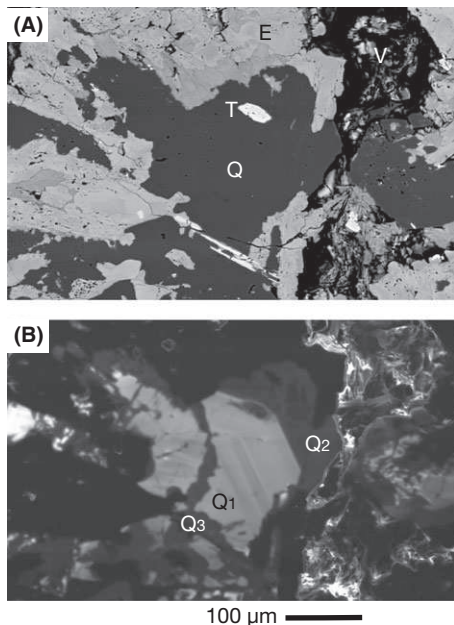


**Fig. 8.** Comparison of back-scattered electron (BSE) and cathodoluminescence (CL) images of the same area of 59133. Much of the image is composed of void-filling epidote and quartz with a small euhedral titanite (T). In A, the variable chemical composition of the epidote is clear. B shows the complexity of the crystallisation of the quartz. The bright areas (Q1) show a growth zoning of the quartz and are rich in Al and Ti compared to the darker areas, which have higher Fe contents (Connell 2000). Dark Q2 quartz overgrows bright Q1 quartz and both Q1 and Q2 are cut by late dark veins (Q3) that seem to be replacing the earlier Q1 and Q2.

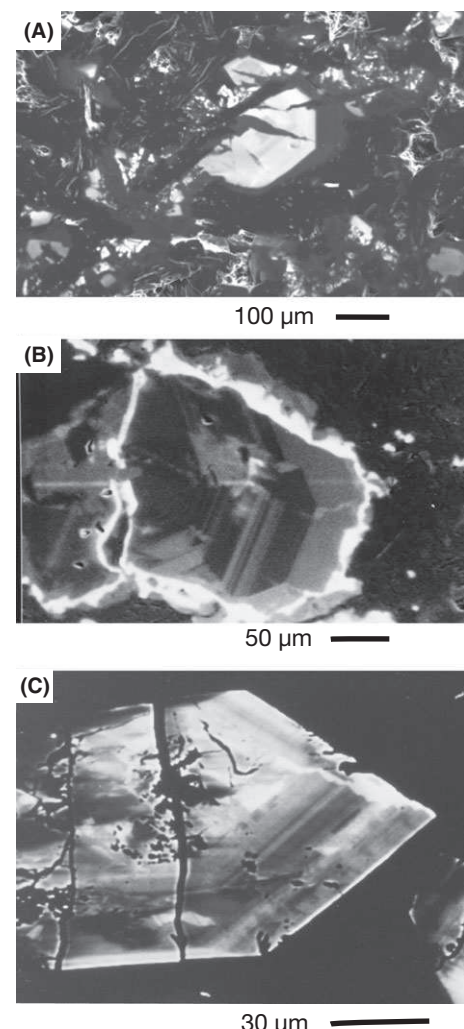


**Fig. 9.** Examples of growth zoning in quartz and epidote. (A) (58508) CL image showing quartz with a bright core surrounded by a dark rim and cut by late replacement quartz and an even later fracture now filled with dark quartz, a similar relation to that of Fig. 8B. (B) (58596) CL image showing a very different sequence of quartz zoning. Here, the early, zoned growth is of dark quartz, surrounded by a thin rim of very bright quartz in turn surrounded by dark quartz again. (C) (59133) BSE image of epidote projecting into a void, showing oscillatory zoning of the composition of the crystal resulting from growth from the circulating fluid. Note that the contrast has been turned up to emphasise zoning in the epidote, so that both quartz and void space are black in this image.

of VMS sulphide deposits within the overlying lava pile. The decreasing number of mineral phases in the series of alteration products between the background sheeted dykes and the epidosites can be linked to the open-system metasomatic model of Korzhinskii (1959, 1965), which predicts that increasing the proportion of infiltrated fluid leads to an increase in the number of mobile components in a system and hence to a decrease in the number of mineral phases present.

The field relations allow this line of evidence to be taken further. If the presence of stripes of epidosites within

individual dykes reflects the variation in the local fluid/rock ratio or mass flux, then the elongation of the stripes parallel to the dyke margins must indicate heterogeneous fluid flow confined at that time within a single dyke. The flow must be linked to the margins of the dyke. This conclusion is confirmed by the continuity of stripes parallel to dyke margins, even when a dyke curves quite sharply, and is consistent with the typically higher degree of alteration of dyke centres relative to the margins. The consistent sharp truncation of the stripes in an older dyke as it is cut by a younger dyke is relevant too. It indicates that the stripes were already present in the older dyke when the younger dyke was intruded and were not modified by the intrusion or by the fluid flow in the younger dyke. Another indicator that the alteration is local rather than regional is the common occurrence of less altered dykes cut by more altered dykes. If the alteration had been regional and gradual then newly intruded dykes would be less altered than older dykes.

Related to this is a further observation; only rarely is epidote seen along the joints that cut across a dyke. In those rare cases, the joints are coated with a thin layer of epidote and quartz, as is often seen in metabasaltic dykes in other types of environment. Much more commonly in the epidosite zones the joints are empty, even when the core of the dyke is clearly striped and must have seen intense fluid–rock interaction. This suggests that, in most cases, the alteration took place before the cross-cutting joints had formed.

### Rapidity of epidotization

The combination of the field evidence summarized here indicates strongly that within an epidosite zone individual dykes are altered soon after they have been intruded, with the intensity of alteration variable both within a dyke and between different dykes. An approximate maximum time-scale for cross-cutting dykes can be calculated as follows. The Valu Fa spreading centre in the Tonga back arc has a similar magma chemistry to that in Troodos (Jenner *et al.* 1987) and has a half spreading rate of 25–30 mm year<sup>-1</sup> (Taylor *et al.* 1996). Given the Valu Fa spreading centre as a model, and a half width of the dyke injection zone at Troodos of <100 m (Kidd 1977), it would take about 3000 years for a dyke intruded close to the centre of the injection zone to spread to the edge of the zone. Effectively, this represents the time taken for the construction of the sheeted dyke complex at any one site. The interval between intrusions of two cross-cutting dykes would be expected to be much shorter than this.

This is the time frame of complete replacement of much of the earlier dyke by new minerals and is extremely rapid by normal metamorphic standards. The rapidity of alteration indicates that the protolith for the epidosites

was not the background dyke material found outside the epidosite zones, but was the primary igneous mineralogy of a newly crystallized dyke. The close association of intrusion and alteration indicates that, to form epidosites, intrusion must have taken place within an active black smoker system.

Flow of hydrothermal fluid through a newly intruded dyke requires the generation of permeability within the dyke, especially given the flow necessary to produce the intense alteration that yields the epidosites. The petrographic evidence summarized above and shown in Figs 4–5 demonstrates that the alteration has generated significant porosity within the epidosite stripes. Some of this porosity still remains, with some pores isolated, and others as a network of cracks. The petrography shows that there was originally much greater porosity (up to 20%) that was subsequently filled by precipitation of epidote, quartz and chlorite.

These substantial changes in mineral assemblage and porosity show that the volume of fluid flow along an epidosite stripe must have been considerable. This alone indicates that the permeability in the stripe must have been high, and thus that the porosity now visible was linked to a network.

### Formation of stripes

How then were the stripes formed? A newly crystallized dyke could have about 10% of grain-scale porosity from an approximate 10% increase in density on solidification of basaltic magma (Hooft & Detrick 1993). In addition, thermal contraction during extremely rapid cooling from 1000 to 400°C could introduce grain boundary cracks. This porosity would be likely to have given rise to a somewhat higher permeability in the new dyke compared with the surrounding older dykes. Black smoker fluid, already flowing through the dyke wall rocks would enter the dyke and start to flow along it. The fluid would immediately start to react with the igneous minerals, potentially increasing the porosity and permeability. Numerical models of this process show that the result would be the development of fingers of altered and permeable material propagating in the direction of fluid flow into unaltered rock (Steefel & Maher 2009). This results from the positive feedback between dissolution rate, fluid flow and permeability. In the case of a dyke intruded into a black smoker upflow zone, this process of fingering will begin simultaneously over a large vertical extent of the dyke. Once the fingers began to link together, the dyke as a whole would become permeable and fluid flow would focus increasingly into it. However, mineral precipitation would be continuously and simultaneously occluding the porosity and reducing the permeability. For this reason, the highest local permeabilities would be at the metasomatic front between altered and

fresh rock; this may provide a mechanism for the initial fingers to coalesce into the sheet-like stripes.

From a geochemical standpoint, the major problem is how a single fluid flow regime such as this could change from giving rise to net dissolution of silicate rock to create porosity to infilling the porosity by silicate precipitation. Creation of this porosity immediately after intrusion requires the rapid dissolution of primary minerals. A black smoker fluid at 350–400°C is likely to be ‘far from equilibrium’ with respect to igneous minerals formed at 1000°C. Typical behaviour is that rates of dissolution increase from zero at equilibrium and then plateau at affinities  $> 60 \text{ kJ mol}^{-1}$  (Brantley *et al.* 2008). Under far from equilibrium conditions, silicate dissolution rates are extremely rapid, particularly at low pH. *In situ*, pH in basalt-hosted black smoker systems is estimated to be about 5 (Pester *et al.* 2012). For example, at 300°C and pH 5, orthopyroxene is predicted to dissolve at  $4.3 \times 10^{-11} \text{ mol cm}^{-2} \text{s}^{-1}$  (Oelkers & Schott 2001) which corresponds to a rate of enlargement of a grain boundary crack or pore of  $1.2 \mu\text{m day}^{-1}$ . Rates at 500°C would be about an order of magnitude faster, and an alteration front could pass through the width of a dyke in about 200 years. In practice, many sites of dissolution would operate simultaneously, and a dyke could be fully altered in much less time than that. Rates for other minerals including clinopyroxene are similar, although rarely measured at higher temperatures (Brantley & Chen 1995; Chen & Brantley 1998; Bandstra *et al.* 2008; Kaszuba *et al.* 2013).

Simple mineral dissolution is a good analogy to capture the general nature of the changes, but fails to account for the overall changes that have taken place. This is because the concentrations of the key rock-forming elements (Si and Al) in black smoker brines are much less than those of Ca, Fe and most other mineral-forming cations (Von Damm 1995), whereas simple mineral dissolution requires that they are dissolved stoichiometrically. The actual dissolution reactions likely involved simultaneous growth of secondary phases. The retention of the original dyke geometry, combined with relict porosity, nevertheless suggests that there has been net removal of material and components such as Na and Mg have been quantitatively removed from the epidosites. In particular, Si was dissolved, but then was returned to the rock as the void space was infilled, but there is no evidence for a significant change in fluid composition or flow regime to account for this change in behaviour. We can propose two alternative end-member hypotheses for the formation of the epidote stripes. It is normally assumed that Si in black smoker systems is buffered at saturation by the presence of quartz (Wells & Ghiorso 1991). In fact, quartz is a rare phase in ocean floor alteration assemblages and recharging fluids may be below quartz saturation, but the abundance of quartz in epidosites suggests that saturation is reached or

exceeded. Si content of black smoker systems is widely used as a geothermometer or geobarometer for the base of hydrothermal flow (Fontaine *et al.* 2009), showing that supersaturation of silica (and by inference other components) is normal during the rapid upflow of black smoker fluids to vents. In view of this, one hypothesis is that the epidote stripes develop as primary igneous minerals rapidly dissolve while their secondary reaction products grow nearby. The reaction is driven by the instability of the primary assemblage under greenschist facies conditions, rather than by gradients in P, T or fluid composition.

The alternative hypothesis is that porosity in any one stripe is variable through time and the sequence of porosity generation followed by infilling reflects cooling of the flow system.

Over a wide range of P-T conditions, silica solubility in gas-poor aqueous fluids increases with pressure and temperature (prograde solubility), but retrograde behaviour occurs at temperatures above the critical point for sea water salinities, in a P-T region which is relevant to epidote formation (Von Damm *et al.* 1991; Akinfiev & Diamond 2009). Steele-MacInnes *et al.* (2012a) showed that dissolution of quartz can occur in the deep upflow part of a black smoker system as the fluid cools in the retrograde solubility region. As the fluid cools further, silica precipitation will occur in the prograde solubility field.

In addition to cooling, silica solubility may also be influenced by pressure fluctuations. These may arise in black smoker systems from a number of causes, such as slip on spreading axis faults or by the precipitation and dissolution of anhydrite as fluid temperature rises and falls (Cann & Strens 1989; Tivey *et al.* 1995).

### Importance of reaction permeability

It is doubtful whether the hydrothermal reaction zone close to the base of a black smoker system has ever been sampled in the modern oceans, but it is also possible that modern reaction zones have a different mineralogy from Cretaceous ones, perhaps due to changes in sea water chemistry. Modern ocean waters have a much higher Mg/Ca ratio than did the oceans of the Cretaceous (Lowenstein *et al.* 2001; Holland 2005; Coogan 2009; Coggon *et al.* 2010). In a modern high-Mg/Ca ocean, the residual phases might be chlorite and quartz, rather than epidote and quartz. Porosity-generating processes similar to those documented here may well exist in systems with different mineralogy. The main driver for the process is the dissolution of primary minerals in black smoker fluid, rather than the precipitation of epidote assemblages per se. This driver is present in any circumstance where fresh igneous minerals come into contact with rapidly flowing black smoker fluids and the reactions between them are far from equilibrium. Depending on whether or not the existence

of a specific range of P-T conditions in which silica has retrograde solubility is also essential (hypothesis 2, above), reaction permeability therefore may be a widespread feature of ocean floor alteration close to the spreading axis; it is probably particularly important in stock works beneath sulphide deposits, see, for example Steele-MacInnes *et al.* (2012b).

We are not suggesting here that reaction permeability replaces fracture permeability as the dominant control on fluid flow in the ocean crust, but that it is a major factor in the development of the most heavily metasomatized rocks in areas where fresh igneous rocks encounter actively flowing hydrothermal fluid. A single dyke forms only a small part of the overall flow system, most of which will be less reactive. In most cases, the increase over fracture permeability caused by reactions would be transient, and while locally very high, might not be able to carry the volume of fluid seen in black smoker discharge. However, each dyke might create a disturbance in the flow pattern and may be a reason for the shifting pattern of venting seen in some well-studied black smoker fields (Rona *et al.* 1993; Kelley *et al.* 2012).

One important aspect of reaction permeability is that it generates positive feedback and thereby allows further fluid access into the reacting parts of the dyke and to previously unreacted minerals. The relatively constant chemistry and high metal content of black smoker fluids requires continuous reaction with fresh hot rock (Pester *et al.* 2012); if fluid flowed only along a network of spaced fractures, this would not be possible, and at temperatures  $<400^{\circ}\text{C}$ , lattice diffusion is too sluggish to deliver components into the fluid even on a grain scale (see, for example Ganguly 2002). The model documented here leads to both rapid and quantified access of fluid to primary minerals and also to continuous mining of remaining fresh rock by the fluid. A continuous access of hydrothermal fluid to fresh basalt is also required by the high  ${}^3\text{He}/{}^4\text{He}$  ratios observed in both black smoker vent fluids and in fresh mid-ocean ridge basalts (Craig & Lupton 1981; Graham *et al.* 1993). Reaction permeability is thus important both to the chemistry of the oceans and the formation of mineral deposits.

### Regional implications

Within the epidote zones are many dykes metamorphosed to the same degree as the regional background alteration outside the epidote zones. These dykes are interpreted here as the result of alteration at a lower flux of hydrothermal fluid than the intense flux that formed the epidotes. The low-degree dykes may be cut by later dykes containing epidote stripes and hence altered at a higher fluid flux. On a wider scale, this is consistent with the model of Coogan (2008) that the regional metamorphism of the sheeted dykes is the result of widespread low-fluid-flux reactions with axial hydrothermal systems. The epido-

sites would thus be the markers of more intense hydrothermal alteration within a broad zone of axial hydrothermal circulation.

### CONCLUSIONS

We have shown that the process of epidotization in the sheeted dyke complex of the Troodos ophiolite was accompanied by the generation of significant porosity, probably at least 20% on the scale of a single thin section. We infer that the primary minerals were dissolved in hydrothermal fluid and then epidote, quartz and sometimes chlorite grew euhedrally into the resulting porosity. Epidote is concentrated into stripes (i.e. bands) parallel to dyke margins, separated by less altered (but still completely recrystallised) rock. Cross-cutting relationships show that each dyke was epidotized before being cut by any later dyke, indicating a maximum timescale of around 2000 years for epidotization and a more likely timescale as little as one tenth this. This requires a rapid self-organizing process. Numerical modelling of similar systems (Steefel & Maher 2009) shows that dissolution-induced permeability is a positive feedback process that leads to the development of porosity wormholes which evolve into fingers of alteration.

We suggest that epidote formed in the lower part of the upflow zone of a black smoker system, above the melt lens that would have supplied heat to the system. A newly intruded dyke would cool very rapidly to the temperature of black smoker fluid,  $350\text{--}400^{\circ}\text{C}$  and subsequently remain at that temperature throughout its vertical extent. The dyke would have a significant initial permeability due to the density increase during crystallization and subsequent rapid cooling from  $1000$  to  $400^{\circ}\text{C}$ . The black smoker fluid would be far from equilibrium with the primary minerals in the dyke and far in excess relative to the volume of the fluid in dyke. In far from equilibrium conditions, experimentally determined dissolution rates of minerals are extremely rapid, with data on clinopyroxene suggesting rates of up to a few microns per day in low-pH fluids at black smoker temperatures. Maintaining far from equilibrium conditions requires a rapidly flowing fluid and therefore a high permeability. Transport of major components in the fluid may have been aided by retrograde solubility in the vicinity of the critical point for  $\text{H}_2\text{O}$ , and perhaps by pressure fluctuations due to the dynamic nature of porous medium convection. As soon as the porosity formed, it would begin to be occluded, and the highest permeability in the system would therefore be at the interface between fresh and altered rock. This gives a mechanism for initial pods of porosity within the dyke to coalesce into layers, forming the characteristic stripes.

Both epidotes and less altered dykes in the Troodos ophiolite are strongly depleted in the metals that are

enriched in massive sulphide deposits. If permeability is restricted to cracks, as is widely assumed, it is extremely difficult for components in primary minerals to be released into the fluid at temperatures <400°C where volume diffusion is extremely sluggish. Reaction permeability provides a mechanism for rapid complete recrystallization, with access of fluid to all parts of the rock. In this respect, it may be a key part of the exchange of components between the lithosphere and the ocean-atmosphere system and the recycling of components back into the mantle at subduction zones.

The critical part of our model is the rapid dissolution of primary minerals in circulating hydrothermal fluid. Reaction permeability may be important in other parts of the ocean crust and in other environments where fresh igneous rocks are brought into contact with hydrothermal fluid. In such environments, the rock alteration may well proceed as rapidly as we demonstrate here, where the alteration takes place in the interval between the intrusion of one dyke and another. This conclusion may shine a different light on many other examples of extreme metasomatism, often assumed to have happened at the slow speeds of continental geology.

## ACKNOWLEDGEMENTS

We are indebted to the work of our students Jonathan Cowan (Newcastle upon Tyne PhD thesis, 1990), Jennifer Connell (Leeds MSc thesis 2000) and Graeme Penwright, who collected and documented large amounts of data on the epidotites of the Troodos ophiolite. This research was partly supported by NERC grant NE/I015035/1 to Andrew McCaig. The authors confirm that they have no conflict of interest.

## REFERENCES

- Adamides NG (1990) Hydrothermal circulation and ore deposition in the Troodos ophiolite, Cyprus. In: *Ophiolites: Oceanic Crustal Analogues* (eds Malpas J, Moores EM, Panayiotou A, Xenophontos C), pp. 685–704. Geological Survey Department, Nicosia, Cyprus.
- Akinfiev NN, Diamond LW (2009) A simple predictive model of quartz solubility in water-salt-CO<sub>2</sub> systems at temperatures up to 1000 °C and pressures up to 1000 MPa. *Geochimica Cosmochimica Acta*, **76**, 1597–1608.
- Baker ET, German CR (2004) On the global distribution of hydrothermal vent fields. In: *Mid-Ocean Ridges: Hydrothermal Interactions between the Lithosphere and Oceans*, Vol.148, (eds German CR, Lin J, Parson LM), pp. 245–66. American Geophysical Union, Washington DC.
- Balashov VN, Yardley BWD (1998) Modeling metamorphic fluid flow with reaction-compaction-permeability feedbacks. *American Journal of Science*, **298**, 441–70.
- Bandstra JL, Buss HL, Campen RK, Liermann LJ, Noore J, Haurath EM, Navarre-Sitchler AK, Jang J-H, Brantley SL, 2008, Compilation of mineral dissolution rates. In: *Kinetics of Water-Rock Interaction* (eds Brantley SL, Kubicki JD, White AF). Springer Verlag.
- Banerjee NR, Gillis KM (2001) Hydrothermal alteration in a modern suprasubduction zone: the Tonga forearc crust. *Journal of Geophysical Research-Solid Earth*, **106**, 21737–50.
- Banerjee NR, Gillis KM, Muehlenbachs K (2000) Discovery of epidotites in a modern oceanic setting, the Tonga forearc. *Geology*, **28**, 151–4.
- Baragar WRA, Lambert MB, Baglow N, Gibson IL (1990) The sheeted dike zone in the Troodos ophiolite. In: *Ophiolites: Oceanic Crustal Analogues* (eds Malpas J, Moores EM, Panayiotou A, Xenophontos C), pp. 37–52. Geological Survey Department, Nicosia, Cyprus.
- Bear LM (1963) *The Mineral Resources and Mining Industry of Cyprus*. Geological Survey Department, Nicosia, Cyprus.
- Becker K, Davis EE (2004) In situ determinations of the permeability of the igneous oceanic crust. In: *Hydrogeology of the Oceanic Lithosphere* (eds Davis E, Elderfield H), pp. 189–224. Cambridge University Press, Cambridge, UK.
- Bettison-Varga L, Varga RJ, Schiffman P. (1992) Relation between ore-forming hydrothermal systems and extensional deformation in the Solea graben spreading center, Troodos ophiolite, Cyprus. *Geology*, **20**, 987–90.
- Bettison-Varga L, Schiffman P, Janecky DR (1995) Fluid-rock interaction in the hydrothermal upflow zone of the Solea graben, Troodos ophiolite, Cyprus. *Geological Society of America Special Papers*, **296**, 81–111.
- Bickle MJ, Teagle DAH (1992) Strontium alteration in the Troodos ophiolite – implications for fluid fluxes and geochemical transport in mid-ocean ridge hydrothermal systems. *Earth and Planetary Science Letters*, **113**, 219–37.
- Bickle MJ, Teagle DAH, Beynon J, Chapman HJ (1998) The structure and controls on fluid-rock interactions in ocean ridge hydrothermal systems: constraints from the Troodos ophiolite. In: *Modern Ocean Floor Processes and the Geological Record*, Vol. 148 (eds Mills RA, Harrison K), pp. 127–52. Geological Society of London, London, UK.
- Brantley SL, Chen Y (1995) Chemical weathering rates of pyroxenes and amphiboles. *Mineralogical Society of America Reviews in Mineralogy and Geochemistry*, Vol. 31, pp. 119–72. Mineralogical Society of America, Chantilly, VA.
- Brantley SL, Kubicki JD, White AF (2008) *Kinetics of Water-Rock Interaction*. Springer Verlag.
- Cann JR, Gillis KM (2004) Hydrothermal insights from the Troodos ophiolite, Cyprus, In: *Hydrogeology of the Oceanic Lithosphere* (eds Davis E, Elderfield H), pp. 274–310. Cambridge University Press, Cambridge, UK.
- Cann JR, Strens MR (1989) Modeling periodic megaplume emission by black smoker systems. *Journal of Geophysical Research*, **94**, 12227–37.
- Chen Y, Brantley SL (1998) Diopside and anthophyllite dissolution at 25 degrees and 90 degrees C and acid pH. *Chemical Geology*, **147**, 233–48.
- Coggan RM, Teagle DAH, Smith-Duque CE, Alt JC, Cooper MJ (2010) Reconstructing past seawater Mg/Ca and Sr/Ca from mid-ocean ridge flank carbonates. *Science*, **327**, 1114–7.
- Connell J (2000) Generation and destruction of porosity during the hydrothermal alteration of the sheeted dike complex in the Troodos ophiolite, Cyprus. MSc (Geochemistry) thesis, University of Leeds.
- Constantinou G, Govett GJS (1972) Genesis of sulphide deposits, ochre and umber of Cyprus. *Transactions of the Institution of Mining and Metallurgy*, **81**, B34–46.
- Constantinou G, Govett GJS (1973) Metallogensis associated with the Troodos ophiolite. *Economic Geology*, **68**, 843–58.

- Coogan LA (2008) Reconciling temperatures of metamorphism, fluid fluxes and heat transport in the upper crust at intermediate to fast-spreading mid-ocean ridges. *Geochemistry, Geophysics, Geosystems*, **9**, doi 10.1029/2007/GC001787.
- Coogan LA (2009) Altered oceanic crust as an inorganic record of palaeoseawater Sr concentration. *Geochemistry, Geophysics, Geosystems*, **10**, doi 10.1029/2008/GC002341.
- Craig H, Lupton JE (1981) Helium and mantle volatiles in the ocean and the oceanic crust. In: *The Sea, Vol 7* (ed. Emiliani E), pp. 391–428. Wiley Interscience, New York, NY.
- Crane K (1987) Structural evolution of the East Pacific Rise axis from 13°10'N to 10°35'N: interpretations from SeaMARC I data. *Tectonophysics*, **136**, 65–92.
- Detrick RS, Buhl P, Mutter J, Orcutt J, Madsen J, Brocher T (1987) Multi-channel seismic imaging of a crustal magma chamber along the East Pacific Rise. *Nature*, **326**, 35–41.
- Di Iorio D, Lavelle JW, Rona PA, Bemis K, Xu G, Germanovich LN, Lowell RP, Genc G (2012) Measurements and models of heat flux and plumes from hydrothermal discharges near the deep seafloor. *Oceanography*, **25**, 168–79.
- Driesner T (2010) The interplay of permeability and fluid properties as a first-order control of heat transport, venting temperatures and venting salinities at mid-ocean ridge hydrothermal systems. *Geofluids*, **10**, 132–41.
- Edwards S, Hudson-Edwards K, Cann J, Malpas J, Xenophontos C (2010) *Cyprus-Classic Geology in Europe 7*. Terra Publishing, Harpenden, UK. ISBN-13: 978-1-903544-15-0.
- Fonneland-Jorgensen H, Furnes H, Muehlenbachs K, Dilek Y (2005) Hydrothermal alteration and tectonic evolution of an intermediate- to fast-spreading back-arc oceanic crust: late Ordovician Solund-Stavfjord ophiolite, western Norway. *Island Arc*, **14**, 517–41.
- Fontaine FJ, Wilcock WSD, Foustaoukos DE, Butterfield DA (2009) A Si–Cl geothermobarometer for the reaction zone of high-temperature, basaltic-hosted midocean ridge hydrothermal systems. *Geochemistry, Geophysics, Geosystems*, **10**, Q05009.
- Francheteau J, Armijo R, Cheminee JL, Hekinian R, Lonsdale P, Blum N (1992) Dike complex of the East Pacific Rise exposed in the walls of Hess Deep and the structure of the upper oceanic crust. *Earth and Planetary Science Letters*, **111**, 109–21.
- Gallahan WE, Duncan RA (1994) Spatial and temporal variability in crystallisation of celadonites within the Troodos ophiolite, Cyprus: implications for low-temperature alteration of the oceanic crust. *Journal of Geophysical Research*, **99**, 3147–61.
- Ganguly J (2002) Diffusion kinetics in minerals: principles and applications to tectono-metamorphic processes. *EMU Notes in Mineralogy*, **4**, 271–309.
- German CR, Lin J (2004) The thermal structure of the oceanic crust, ridge-spreading and hydrothermal circulation: how well do we understand their inter-connections? In: *Mid-Ocean Ridges: Hydrothermal Interactions between the Lithosphere and Oceans* (eds German CR, Lin J, Parson LM), AGU Geophysical Monograph Series, **148**, 1–18.
- Graham DW, Christie DM, Harpp KS, Lupton JE (1993) Mantle-plume helium in submarine basalts from the Galapagos Platform. *Science*, **262**, 2023–6.
- Harper GD, Bowman JR, Kuhns R (1988) A field, chemical and stable isotope study of subseafloor metamorphism of the Josphine ophiolite, California-Oregon. *Journal of Geophysical Research*, **93**, 4625–56.
- Holland HD (2005) Sea level, sediments and the composition of seawater. *American Journal of Science*, **305**, 220–39.
- Hooft EEE, Detrick RS (1993) The role of density in the accumulation of basaltic melts at mid-ocean ridges. *Geophysical Research Letters*, **20**, 423–6.
- Huang R, Audétat A (2012) The titanium-in-quartz (TitaniQ) thermobarometer: a critical examination and re-calibration. *Geochimica et Cosmochimica Acta*, **84**, 75–89.
- Humphris SE, Cann JR (2000) Constraints on the energy and chemical balances of the modern TAG and ancient Cyprus seafloor sulfide deposits. *Journal of Geophysical Research*, **105**, 28477–88.
- Ingebretsen SE, Geiger S, Hurwitz S, Driesner T (2010) Numerical simulation of magmatic hydrothermal systems. *Reviews of Geophysics*, **48**, RG1002.
- Jenner GA, Cawood PA, Rautenschlein M, White WM (1987) Composition of back-arc basin volcanics, Valu Fa Ridge, Lau Basin – evidence for a slab-derived component in their mantle source. *Journal of Volcanology and Geothermal Research*, **32**, 209–22.
- Jowitt SM, Jenkin GRT, Coogan LA, Naden J (2012) Quantifying the release of base metals from source rocks for volcanogenic massive sulfide deposits: effects of protolith composition and alteration mineralogy. *Journal of Geochemical Exploration*, **118**, 47–59.
- Juteau T, Manac'h O, Lécuyer C, Ramboz C (2000) The high-temperature reaction zone of the Oman ophiolite: new field data, microthermometry of fluid inclusions, PIXE analyses and oxygen isotopic ratios. *Marine Geophysical Researches*, **21**, 351–85.
- Kaszuba J, Yardley BWD, Andreani M (2013) Experimental perspectives of mineral dissolution and precipitation due to carbon dioxide – water – rock interactions. *Reviews in Mineralogy & Geochemistry*, **77**, 153–88.
- Kelley DS, Carbotte SM, Caress DW, Clague DA, Delaney JR, Gill JB, Hadaway H, Holden JF, Hooft EEE, Kellogg JP, Lilley MD, Stoermer M, Toomey D, Weekly R, Wilcock WSD (2012) Endeavour Segment of the Juan de Fuca Ridge: one of the most remarkable places on Earth. *Oceanography*, **25**, 44–61.
- Kidd RGW (1977) A model for the process of formation of the upper oceanic crust. *Geophysical Journal of the Royal Astronomical Society*, **50**, 149–83.
- Kidd RGW, Cann JR (1974) Chilling statistics indicate an ocean-floor spreading origin for the Troodos complex, Cyprus. *Earth and Planetary Science Letters*, **24**, 151–5.
- Korzhinskii DS (1959) *Physicochemical Basis of the Analysis of the Paragenesis of Minerals*, 142 pp. Consultants Bureau, New York.
- Korzhinskii DS (1965) The theory of systems with perfectly mobile components and processes of mineral formation. *American Journal of Science*, **263**, 193–205.
- Lister CRB (1974) On the penetration of water into hot rock. *Geophysical Journal International*, **39**, 465–509.
- Little CTS, Cann JR, Herrington RJ, Morisseau M (1999) Late Cretaceous hydrothermal vent communities from the Troodos ophiolite, Cyprus. *Geology*, **27**, 1027–30.
- Lowell RP, Germanovich LN (2004) Hydrothermal processes at mid-ocean ridges: results from scale analysis and single-pass models. In: *Mid-Ocean Ridges: Hydrothermal Interactions between the Lithosphere and Oceans*, Vol.148, (eds German CR, Lin J, Parson LM), pp. 219–44. American Geophysical Union Washington DC.
- Lowenstein TK, Timofeef MO, Brennan ST, Hardie LA (2001) Oscillations in Phanerozoic seawater chemistry: evidence from fluid inclusions. *Science*, **294**, 1086–8.
- Nehlig P, Juteau T (1988) Flow porosities, permeabilities and preliminary data on fluid inclusions and fossil thermal gradients

- in the crustal sequence of the Semail ophiolite (Oman). *Tectonophysics*, **151**, 199–221.
- Nehlig P, Juteau T, Bendel V, Cotten J (1994) The root zones of oceanic hydrothermal systems – constraints from the Samail Ophiolite (Oman). *Journal of Geophysical Research*, **99**, 4703–13.
- Oelkers EH, Schott J (2001) An experimental study of enstatite dissolution rates as a function of pH, temperature, and aqueous Mg and Si concentration, and the mechanism of pyroxene/pyroxenoid dissolution. *Geochimica et Cosmochimica Acta*, **65**, 1219–31.
- Pearce JA, Lippard SJ, Roberts S (1984) Characteristics and tectonic significance of supra-subduction zone ophiolites. *Geological Society of London Special Publications*, **16**, 77–94.
- Pester NJ, Reeves EP, Rough ME, Ding K, Seewald JS, Seyfried WE (2012) Subseafloor phase equilibria in high-temperature hydrothermal fluids of the Lucky Strike Seamount (Mid-Atlantic Ridge, 37°17'N). *Geochimica et Cosmochimica Acta*, **90**, 303–22.
- Quon SH, Ehlers EG (1963) Rocks of the northern part of the Mid-Atlantic Ridge. *Geological Society of America Bulletin*, **74**, 1–7.
- Richardson CJ, Cann JR, Richards HG, Cowan JG (1987) Metal-depleted root zones of the Troodos ore-forming hydrothermal systems, Cyprus. *Earth and Planetary Science Letters*, **84**, 243–53.
- Rona PA, Hannington MD, Raman CV, Thompson G, Tivey MK, Humphris SE, Lalou C, Petersen S (1993) Active and relict seafloor hydrothermal mineralization at the TAG hydrothermal field, Mid-Atlantic Ridge. *Economic Geology*, **88**, 1989–2017.
- Schiffman P, Smith BM (1988) Petrology and oxygen isotope geochemistry of a fossil seawater hydrothermal system within the Solea graben, northern Troodos ophiolite, Cyprus. *Journal of Geophysical Research*, **93**, 4612–24.
- Schiffman P, Smith BM, Varga RJ, Moores EM (1987) Geometry, conditions and timing of off-axis hydrothermal metamorphism and ore-deposition in the Solea graben. *Nature*, **325**, 423–5.
- Scott RB, Rona PA, McGregor BA, Scott MR (1974) The TAG hydrothermal field. *Nature*, **251**, 301–2.
- Shand SJ (1949) Rocks of the mid-Atlantic ridge. *Journal of Geology*, **57**, 89–92.
- Staudigel H, Gillis K, Duncan R (1986) K/Ar and Rb/Sr ages of celadonites from the Troodos ophiolite, Cyprus. *Geology*, **14**, 72–5.
- Steefel CI, Maher K (2009) Fluid-rock interaction: a reactive transport approach. In: *Thermodynamics and Kinetics of Water-Rock Interaction*, Vol. 70 (eds Oelkers EH, Schott J), pp. 87–124, Mineralogical Society of America, Chantilly, VA, USA.
- Steele-MacInnes M, Han L, Lowell RP, Rimstidt JD, Bodnar RJ (2012a) The role of fluid phase immiscibility in quartz dissolution and precipitation in sub-seafloor hydrothermal systems. *Earth Planetary Science Letters*, **321–322**, 139–51.
- Steele-MacInnes M, Han L, Lowell RP, Rimstidt JD, Bodnar RJ (2012b) Quartz precipitation and fluid inclusion characteristics in sub-seafloor hydrothermal systems associated with volcanogenic massive sulphide deposits. *Central European Journal of Geosciences*, **4**, 275–86.
- Taylor B, Zellmer K, Martinez F, Goodliffe Andrew (1996) Seafloor spreading in the Lau back-arc basin. *Earth and Planetary Science Letters*, **144**, 35–40.
- Teagle DAH, Alt JC, Halliday AN (1998) Tracing the evolution of hydrothermal fluids in the upper oceanic crust: Sr-isotopic constraints from DSDP/ODP Holes 504B and 896A. In: *Modern Ocean-Floor Processes and the Geological Record*, Vol. 148 (eds Mills RA, Harrison K), pp. 81–97. Geological Society of London, London, UK.
- Tivey MK, Humphris SE, Thompson G, Hannington MD, Rona P (1995) Deducing patterns of fluid flow and mixing within the TAG active hydrothermal mound using mineralogical and geochemical data. *Journal of Geophysical Research*, **100**, 12527–55.
- Valsami E, Cann JR (1992) Mobility of rare earth elements in zones of intense hydro- thermal alteration in the *Pindos ophiolite*, Greece. In: *Ophiolites and Their Modern Oceanic Analogues*, Vol. 60 (ed. Parson LM), pp. 219–32. Geological Society of London, London, UK.
- Van Ark E, Detrick RS, Canales JP, Carbotte SM, Harding AJ, Kent GM, Nedimovic MR, Wilcock WSD, Diebold JB, Babcock J (2007) Seismic structure of the Endeavour segment, Juan de Fuca Ridge: correlations with seismicity and hydrothermal activity. *Journal of Geophysical Research*, **112**, B02401.
- Varga RJ, Gee JS, Bettison-Varga L, Anderson RS, Johnson CE (1999) Early establishment of hydrothermal systems during structural extension; palaeomagnetic evidence from the Troodos ophiolite, Cyprus. *Earth and Planetary Science Letters*, **171**, 221–35.
- Von Damm K (1995) Controls on the chemistry and temporal variability of seafloor hydrothermal fluids. In: *Seafloor Hydrothermal Systems*, Vol. 91 (eds Humphris SE, Zierenberg RA, Mullineaux LS, Thomson RE), pp. 222–47. American Geophysical Union, Washington DC.
- Von Damm KL, Bischoff JL, Rosenbauer RJ (1991) Quartz solubility in hydrothermal seawater; an experimental study and equation describing quartz solubility for up to 0.5 M NaCl solutions. *American Journal of Science*, **291**, 977–1007.
- Wark DA, Watson EB (2006) TitaniQ: a titanium-in-quartz geothermometer. *Contributions to Mineralogy and Petrology*, **152**, 743–54.
- Wells JT, Ghiorso MS (1991) Coupled fluid flow and reaction in mid-ocean ridge hydrothermal systems; the behavior of silica. *Geochimica et Cosmochimica Acta*, **55**, 2467–81.
- Wilson RAM (1959) *The Geology of the Xeros-Troodos Area*. Geological Survey Department Memoir 1. Geological Survey Department, Nicosia, Cyprus.
- Yardley BWD, Lloyd GE (1989) An application of cathodoluminescence microscopy to the study of textures and reactions in high grade marbles from Connemara, Ireland. *Geological Magazine*, **126**, 333–7.
- Yardley BWD, Rochelle CA, Barnicoat AC, Lloyd GE (1991) Oscillatory zoning in metamorphic minerals: an indicator of infiltration metasomatism. *Mineralogical Magazine*, **55**, 357–65.